D. JĘDRZEJCZYK*

EFFECT OF HIGH TEMPERATURE OXIDATION ON STRUCTURE AND CORROSION RESISTANCE OF THE ZINC COATING DEPOSITED ON CAST IRON

WPŁYW WYSOKO-TEMPERATUROWEGO UTLENIANIA NA STRUKTURĘ I ODPORNOŚĆ KOROZYJNĄ POWŁOKI CYNKOWEJ NANIESIONEJ NA ŻELIWO

The presented work describes results regarding influence of the high-temperature oxidation on anticorrosion properties of zinc coating created during hot-dip galvanizing at surface of cast iron contained different graphite precipitates: flake, vermicular, nodular. Test was made in Na_2SO_4 solution, using specific samples in form of cylinder, with groove lathed at the whole side wall circumference, to make the oxidation and galvanizing easier. Before corrosion test, samples were oxidized at temperature 850 °C, within 4h, sandblasted and etched chemically. For comparison, the corrosion resistance of cast iron samples without preliminary oxidation treatment and steel sample galvanized in analogical conditions were also measured. Research confirmed that to obtain subsurface composite cast iron layer two stage scale removal process is necessary: sandblasting combined with chemical treatment. When only sandblasting is applied the clean outside surface is achieved but zinc penetration depth inside after-graphite voids is slight. On the other hand, using one stage chemical treatment the completely removal of relatively thick outside scale layer was impossible. Research proved that cast iron oxidation process increases essentially the corrosion resistance of created zinc layer. This difference changes with dependence on graphite shape and is the smallest in case of nodular graphite and increases as graphite precipitates change to vermicular and flake. The achieved effect results from neutralization of negative influence of graphite precipitation on compactness and continuity of zinc coating and created subsurface composite layer.

Keywords: cast iron oxidation, zinc coating, corrosion resistance

W pracy opisano wyniki badań dotyczących wpływu wysokotemperaturowego utleniania na właściwości antykorozyjne powłoki cynkowej naniesionej podczas cynkowania zanurzeniowego na żeliwo zawierające różną postać grafitu (płatkowy, wermikularny, kulkowy). Badania prowadzono w roztworze Na_2SO_4, na specyficznych próbkach w kształcie walca, z rowkiem wykonanym na całym obwodzie pobocznicy, w celu ułatwienia procesu utleniania i cynkowania. Przed badaniami korozyjnymi próbki utleniano w temperaturze 850 °C, przez okres 4h, po czym piaskowano i chemicznie trawiono. Dla porównania odporność korozyjną określano również na próbkach niepoddanych utlenianiu oraz na próbce stalowej cynkowanej analogicznie. Badania potwierdziły, że do wytworzenia podpowierzchniowej kompozytowej warstwy żeliwa konieczne jest zastosowanie dwuetapowego procesu usuwania zgorzeliny: piaskowania połączonego z obróbką chemiczną. Zastosowanie tylko piaskowania gwarantuje wprawdzie uzyskanie czystej powierzchni zewnętrznej, natomiast głębokość penetracji cynku w głąb pustek po-grafitowych jest znikoma. Z kolei, za pomocą stosowanej obróbki chemicznej całkowite usunięcie relatywnie grubej zewnętrznej warstwy zgorzeliny nie było możliwe. Badania wykazały, że proces utleniania żeliwa w znacznym stopniu zwiększa odporność korozyjną nanoszonej powłoki cynkowej. Różnica zmienia się w zależności od kształtu grafitu i jest najmniejsza w przypadku grafitu kulkowego, i zwiększa się w miarę przechodzenia do grafitu wermikularnego i płatkowego. Uzyskany efekt wynika z neutralizacji szkodliwego wpływu grafitu na zwartość i ciągłość powłoki cynkowej oraz wytworzonej podpowierzchniowej warstwy kompozytowej.

1. Introduction

The hot-dip zinc galvanizing is the most wide applied process of protection of steel and cast iron against negative influence of environment [1, 2]. Therefore a lot of information exists in literature regarding the mechanism of coating growth and optimization of different treatment parameters [3-7]. The structure and properties of zinc coating are dependent on different factors: bath chemical composition, bath temperature level, chemical composition of the base material, etching and fluxing specificity. Process of coating growth affects its corrosion resistance. It is well known that additives of such elements, like: iron, nickel, copper and noble metals

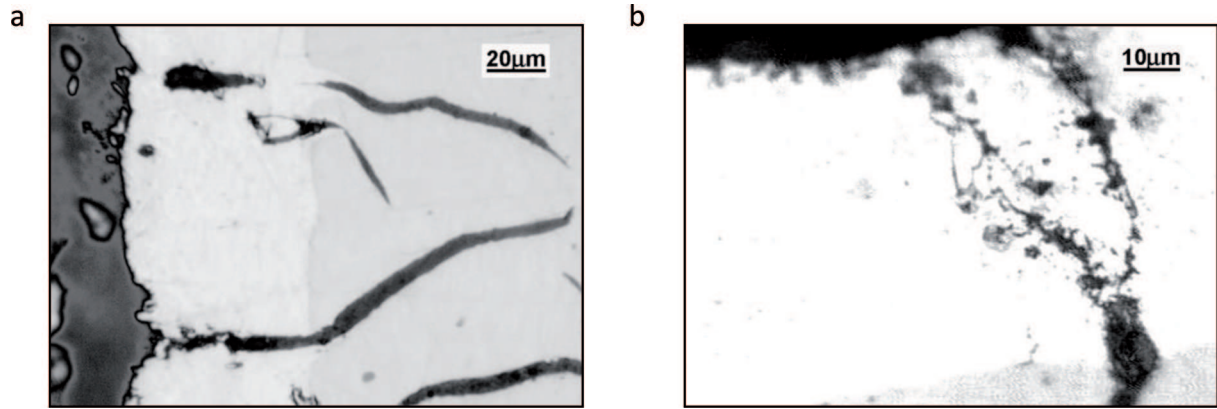* UNIVERSITY OF BIELSKO-BIAŁA, 43-309 BIELSKO-BIAŁA, 2 WILLOWA STR., POLAND

a

b

Fig. 1. Graphite precipitates observed inside the zinc coating created at machined cast iron surface: a – subsurface layer of cast iron; b – the cross section of created zinc coating (own investigation)

increases corrosion rate of zinc in acidic environment. On the other hand, cadmium, led, mercury decreases corrosion rate [8]. In industrial atmosphere (with SO_2) corrosion resistance of zinc coating depends on structure of surface layer and properties of corrosion products – hydroxy – sulphates.

Cast iron is more and more frequent protected in similar way like steel because this widely undervalued material demonstrates sometimes even higher properties than steel (ADI, vermicular cast iron) [9]. Effect achieved during hot-dip zinc galvanizing of cast iron differs essentially from steel. When the content of silicon exceeds level expressed by equation: $(Si+2,5P) \cdot 10^3 = E_{Si,P}$ (170% for "Technigalva" process), thick, brittle and dull-grey coating is created [2, 10]. Excessive coating growth of Zn on steel with Si content in the range 0,03-0,12% is called Sandelin's effect [11], when the silicon content is higher than 0,4% observed process is defined as Guttman-Niessen effect [12]. Moreover, mechanism of zinc layer growth on the high-silicon steel surface differs

from the mechanism of the protecting layer growth on iron casting surface [13](different values of exponent "n" in exponential rule of the growth rate: $\lambda = K \cdot t^n$, where λ– layer's thickness; K – growth rate constant; t – time of treatment; n – constant of the growth rate). Additionally graphite precipitations included in cast iron can penetrate inside the zinc coating decreasing its continuity and tightness (Fig. 1). Literature data confirms also that type of surface pre-treatment effects on corrosion properties of zinc coating [14].

The presented paper is the continuation of investigations [15], where the high temperature oxidation was suggested as the preliminary treatment of cast iron being hot-dip galvanized, that allows for: formation of the composite subsurface layer (metallic matrix-zinc); increasing of Zn diffusion depth; formation of outside Zn layer without graphite precipitation and impurities; increasing of coating quality expressed by relatively low surface roughness (Fig. 2).
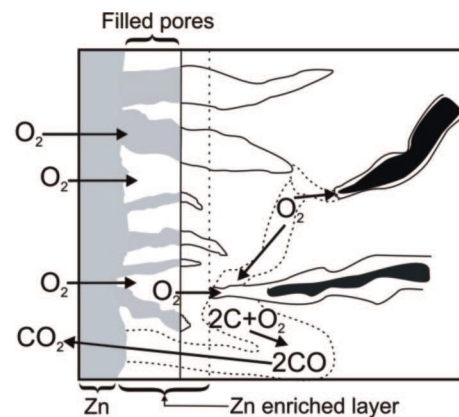

Fig. 2. Effects achieved as the result of high-temperature oxidation of cast iron [15]

Results of already made investigations allow supposing that corrosion resistance of such created coating should be better than resistance of the layer put without high-temperature oxidation. So, the aim of presented work was to verify the effectiveness of proposed method with reference to the zinc coating corrosion resistance.

2. Experimental

Experiment was composed of the following stages: proper *sample preparation* (casting, oxidation, zinc coating), *samples surface analyse* and *corrosion tests. Sample preparation* – investigations refers to cast iron with flake, vermicular and nodular graphite melted in induction furnace of medium frequency. Liquid metal was cast to sand mould with dimensions φ30×300mm (cast iron with flake and vermicular graphite) and Y2 ingots (cast iron with nodular graphite). The chemical composition of cast iron was typical for alloy's grade, i.e.: 3,32%C; 1,80%Si; 0,55%Mn; 0,065%P; 0,035%S (cast iron with flake graphite), 3,63%C; 2,55%Si; 0,10%Mn; 0,025%P; 0,007%S; 0,045%Mg (cast iron with nodular graphite), 3,65%C; 2,58%Si; 0,08%Mn; 0,023%P; 0,008%S; 0,025%Mg, 0,015%Ce (cast iron with vermicular graphite). From such cast ingots cylindrical samples φ =14,7mm, thickness h= 7mm with groove lathed at the whole side wall circumference were turned. Then samples were put to silite furnace PSK 600/25 to oxidize.

The experiment was led in 850°C. Samples have been taken out from the furnace separately after 4 hours. Before oxidation and after cooling dawn samples were exactly measured, weighed, and metallographic specimens were prepared to observe surface perpendicular to sample's axis. The scale layer was removed in two stage procedure: mechanically by sandblasting, as well as chemically, by dipping in solution of oxalic acid. After scale layer removal the hot dip zinc coating in industrial conditions has carried out. Process consisted of the following action: degreasing – dirt and oil removal; pickling – rust, scale and carbon deposit removal; rinsing – hydrochloric acid removal; fluxing – increasing of zinc adhesion to alloy; galvanizing in temperature 460°C, within t=1min in bath enriched with Ni, Bi and Al; cooling – decreasing of sample temperature. *Surface analyse* – to optical observation microscope "NEOPHOT 2" as well as "Axiovert A -100" were applied, whereas further examination was made with application of scanning microscope "Jeol J7" and X-ray analyzer "JCXA – JEOL". Sample's surface quality was described additionally by roughness measurements made after scale layer removal – „MAHR" profile measurement gauge with "Perthometer Concept" software. *Corrosion tests* – corrosion resistance was evaluated using cylindrical samples, by application of potentiostat SI 1286 that enables registration of polarization curves in three electrodes system. Before measure start, samples were placed in corrosion solution – 0,5M Na_2SO_4, in temperature 25°C, within 24h. Samples were subjected to polarization in the same solution, from potential 1000mVNEK in anode direction, with rate 1mV/s. Results were compared to these measured in Zn coated steel (30MnB4 – $E_{Si,P}$ = 60) and cast iron galvanized without high temperature oxidation.
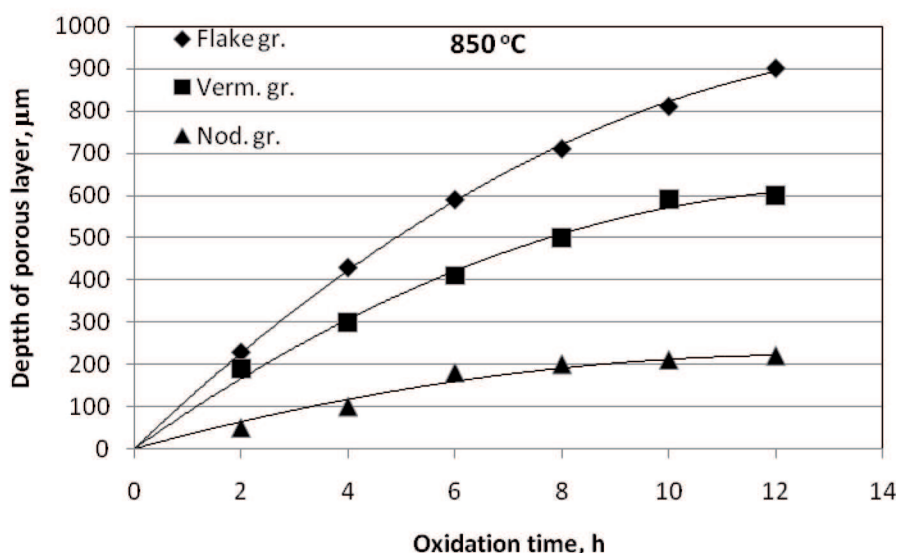

Fig. 3. The influence of graphite shape on cast iron oxidation kinetic in 850°C
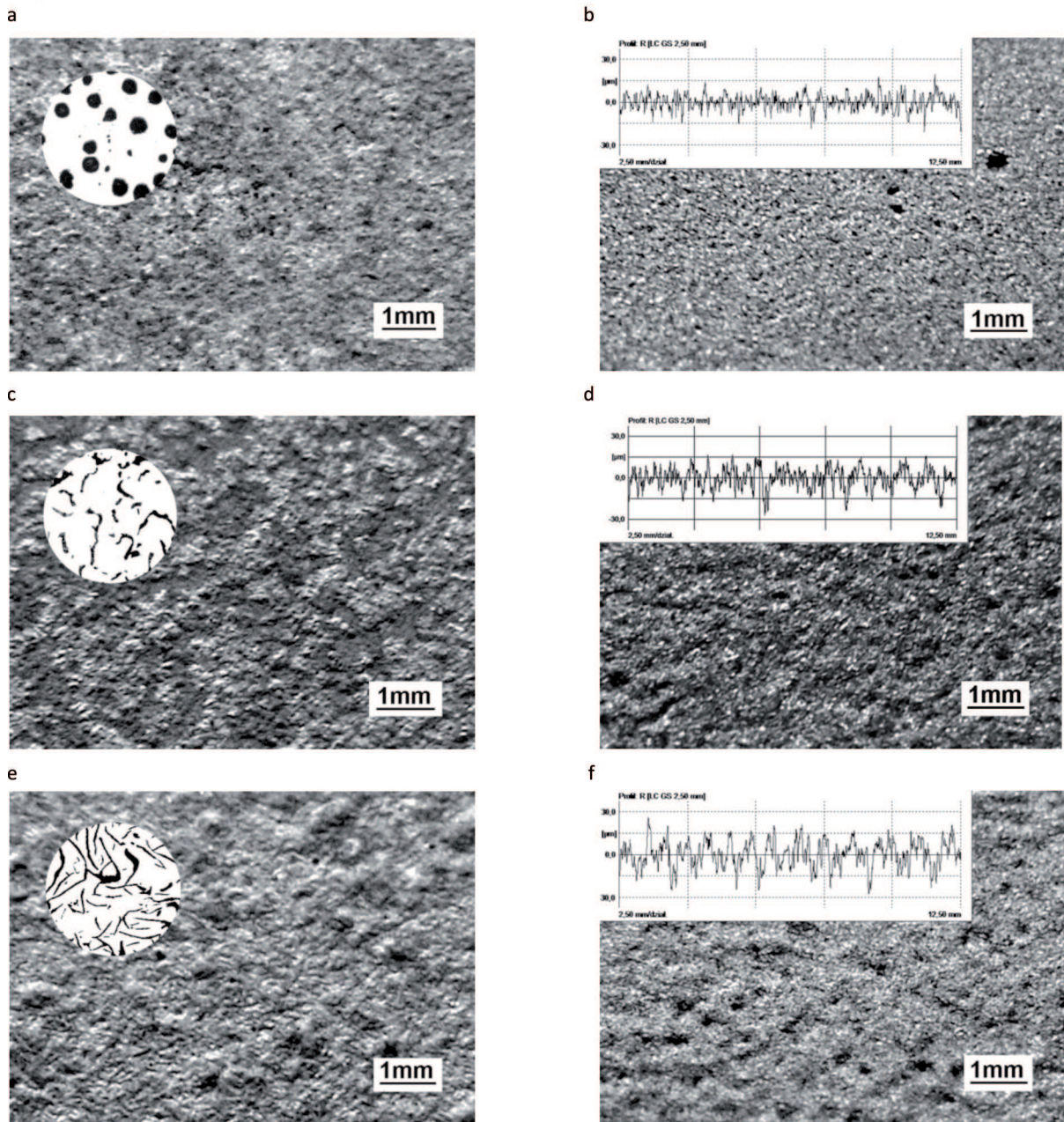
Fig. 4. The view of outside surface of investigated samples with different graphite shape after oxidation (a, c, e) and sandblasting (b, d, f); b – R_a = 4,00μm; d – R_a = 5,76μm; f – R_a = 7,46μm

3. Analysis of results

It results from dependence presented at Fig. 3 that porous layer thickness can be controlled by suitable selection of temperature and the time of oxidation as well as it depends on graphite shape existing in cast iron. Porous layer thickness decreases when graphite shape is changing from flake to vermicular and nodular.

Parameters of oxidation process (T=850°C, t = 4h) were set basic upon the presented relation at the level that, on the one hand guarantees the creation of subsurface porous layer with thickness higher than 120 μm, on the other hand ensures relatively low surface roughness (Figs 3, 4). As an effect of conducted oxidation the samples surface was covered with scale layer with thickness from 40μm (cast iron with nodular graphite) to 200 μm in case of cast iron with flake graphite (Fig. 5).
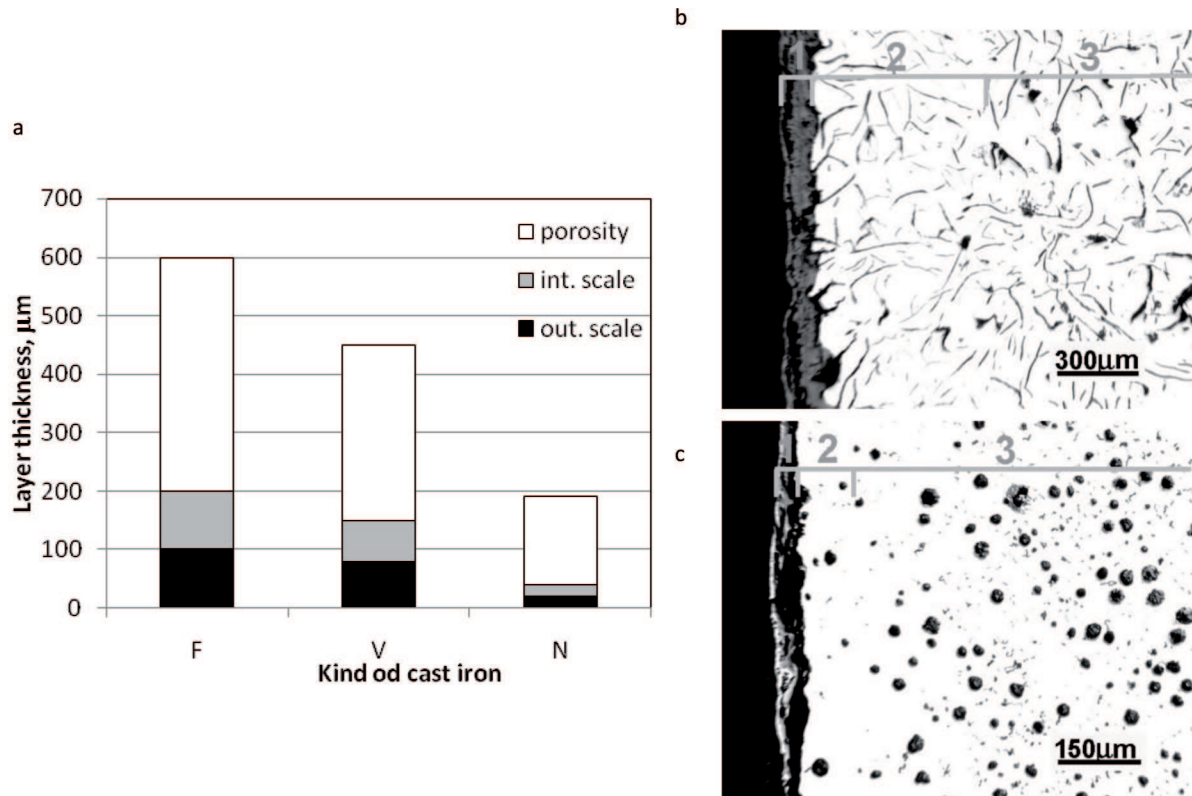
Fig. 5. The thickness of layers created in different cast iron (F – flake graphite; V – vermicular graphite; N – nodular graphite) – a and samples subsurface layer cross section: b – cast iron with flake graphite; c – cast iron with nodular graphite; 1 – scale layer; 2 – decarburized zone; 3 – typical cast iron microstructure
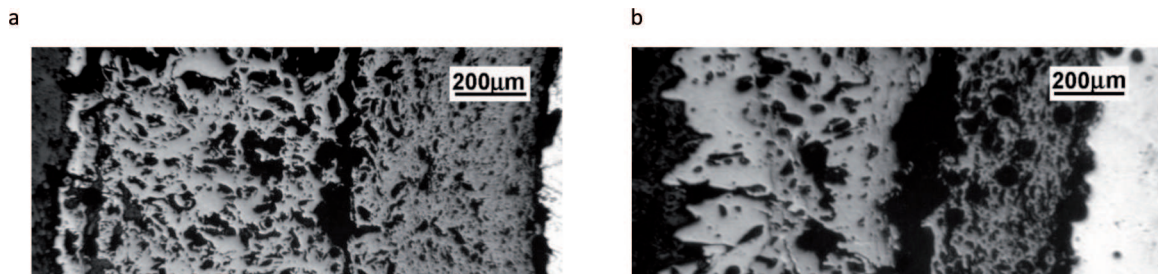

Fig. 6. The cross section of scale observed in cast iron oxidized at 1050°C within 12h: a – with flake graphite; b – with nodular graphite

Also thickness of decarburized layer achieved in established for comparison constant oxidation parameters is not identical and changes from 190 μm in nodular cast iron to 600 μm in cast iron with flake graphite. In practice, applied parameters should be dependent on kind of cast iron – in case of studied materials, where creation of porous layer with thickness close to 200 μm was sufficient, application of oxidation time amounting to t = 2; 2,5 and 8h, correspondingly to cast iron with flake, vermicular and nodular graphite should guarantee better surface quality and higher corrosion resistance of created coating. It means possibility of shortening the oxidation time in the case of flake and vermicular graphite and necessity of extending this time in case of nodular cast

iron. The structure presented at Fig. 5 also confirms necessity of extending the time of oxidation of nodular cast iron because although decarburizing effect is visible at 190μm depth, single precipitates of nodular graphite are observed very close to the surface.

The scale layer created at cast iron surface differs depending on the graphite shape both in terms of macro, as well as micro structure. The most compact structure is observed at nodular cast iron surface. The scale created at the surface of cast iron with vermicular and flake graphite demonstrates the much greater porosity (Fig. 6). This is one of factors which directly influence on oxidation rate and in the process on roughness of treated surfaces. Therefore the most uneven surface was achieved
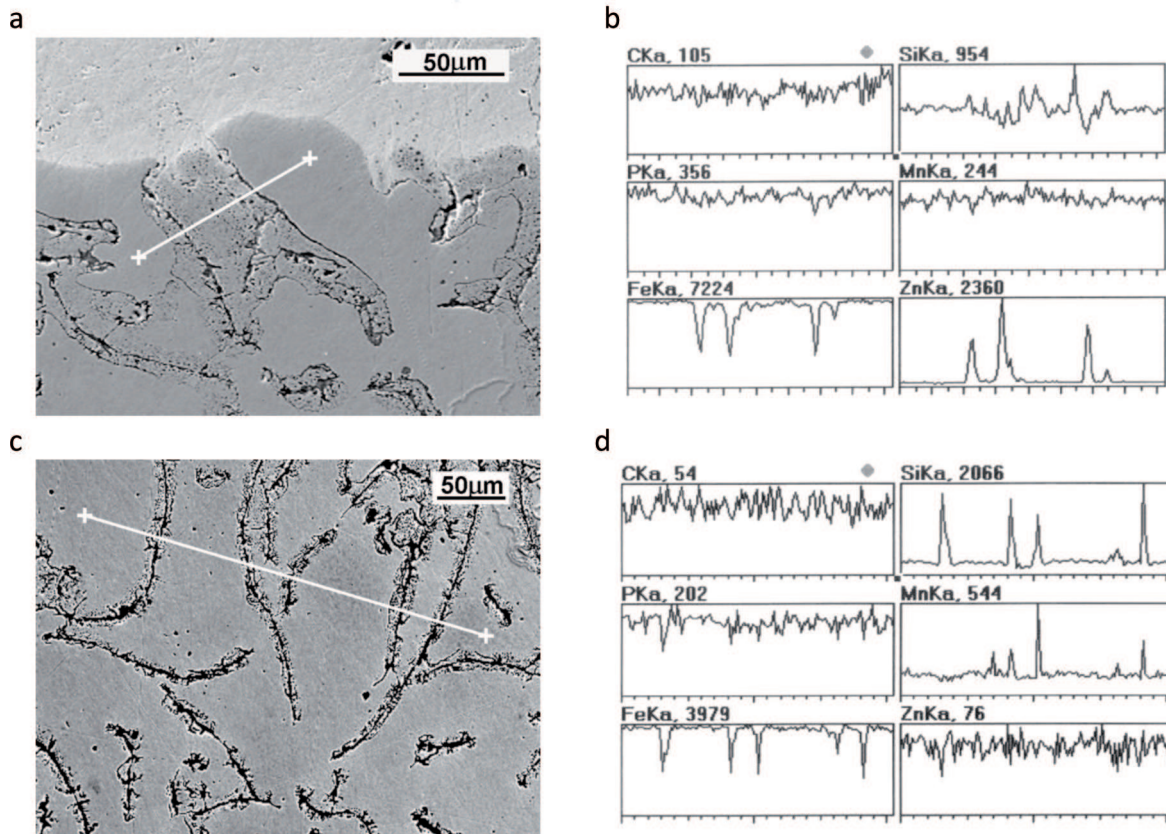
150

Fig. 7. The cross section of subsurface layer of oxidized and galvanized cast iron with RTG linear analysis: a, b – 50μm depth; c, d – 200μm depth

in case of cast iron with flake graphite (R_a =7,46μm). In cast iron with vermicular graphite intermediate roughness values were measured (R_a =5,76μm), whereas the most smooth surface was observed in case of nodular cast iron (R_a =4,00μm). The above described process differentiation results mainly from diverse graphite morphology: nodular graphite particles are separated, whereas vermicular and flake are connected to each other. Apart from that, diversifying of decarburizing and oxidation rate of tested cast iron results also from different chemical composition. In terms of chemical composition the essential difference exists between cast iron with flake graphite and nodular, as well as vermicular cast iron and refers to lower content of silicon (about 0,8%) and higher content of Mn, P and S. The element that plays the major role both during oxidation, as well as during the growth of zinc coating is silicon. On one hand silicon favours the decrease of the rate oxidation, both during external, as well as internal corrosion. On the other hand silicon decreases the Zn coating quality (Sandeline and Guttman-Niessen effects). Cast iron oxidized at high temperature forms at the surface the scale layer that is composed of three zones: wustite (FeO), magnetite (Fe_3O_4) and hematite (Fe_2O_3). Internal scale layer is additionally enriched in fayalite (Fe_2SiO_4) that

increases protecting properties of created scale. Similar filler structure was observed inside "after graphite" pores after oxidation – Fig. 7. The presented cross section and RTG linear analysis confirms that created voids situated very close to the surface are free from graphite and enriched with Zn, whereas the phase identified in pores observed at higher distance are filled with complex Si, Mn compounds.

During the investigation diverse methodology of scale removal was used: sandblasting, chemical etching, sandblasting with etching. Everyone from one stage treatment was insufficient. Chemical etching didn't provide getting enough cleaned surface. Next, after sandblasting the surface was admittedly free from corrosion products but „after graphite pores" were still filled with oxidation products. Only the combination of sandblasting with proper chemical etching enabled the right cleaning of the outside surface and creation internal pores free from oxidation products.

The above mentioned factors affect Zn coating formation at cast iron surface during hot-dip galvanizing and its corrosion resistance. Thickness of zinc layer that was created at the surface of cast iron samples is stable and reaches 70-100μm. Additionally, zinc galvanizing decreases the roughness of tested samples. For exam-

ple, roughness measured at sample with flake graphite, that was oxidized before zinc coating gained value R_a = 3,72μm. It means decreasing in comparison to oxidized surface after sand blasting about 3,74μm. Although R_a values measured after Zn coating don't differ essentially (R_a = 4,11μm – sample galvanized without oxidation), it is visible that roughness obtaining at the surface galvanized after machining is higher than this one measured after galvanizing treatment combined with oxidation.

Fig. 8 presents the comparison of polarization curves determined in case of oxidized cast iron and cast iron galvanized after machining without oxidation. Results were analysed in pairs to enable easier evaluation of oxidation influence. Whereas, at Fig. 9 all registered curves are compared. Because of wide range of registered values the logarithmic scale was used at current density axis.

TABLE 1

Electrochemical parameters measured during experiment

Sample designation	E_{corr} [mV]	E_{K-A} [mV]	R_p [Ωcm^2]	i_{corr} [A/cm^2]
Steel 30MnB4	-672	-675	$8{,}39 \cdot 10^4$	$3{,}11 \cdot 10^{-7}$
FGM	-1070	-1296	$6{,}78 \cdot 10^2$	$3{,}84 \cdot 10^{-5}$
FGO	-371	-517	$5{,}07 \cdot 10^4$	$5{,}14 \cdot 10^{-7}$
VGM	-1050	-1204	$6{,}68 \cdot 10^3$	$3{,}91 \cdot 10^{-6}$
VGO	-389	-407	$8{,}16 \cdot 10^5$	$3{,}19 \cdot 10^{-8}$
NGM	-484	-549	$4{,}95 \cdot 10^5$	$5{,}27 \cdot 10^{-8}$
NGO	-543	-580	$9{,}59 \cdot 10^5$	$2{,}72 \cdot 10^{-8}$

FG – flake graphite, VG – vermicular graphite, NG – nodular graphite; „M" – machined, „O" – oxidized
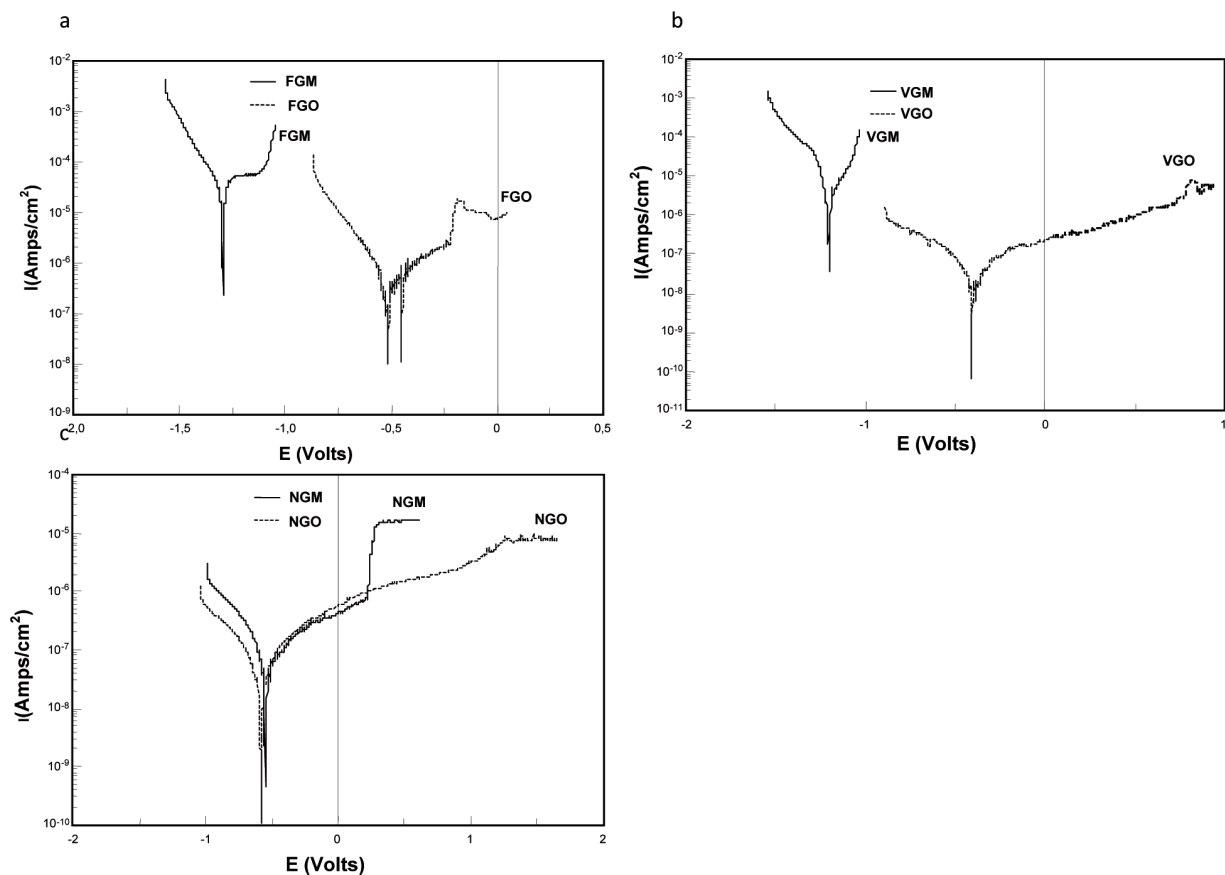

Fig. 8. Polarization curves registered in case of cast iron: with flake graphite (FG) – a, with vermicular graphite (VG) – b and nodular graphite (NG) – c; „O" – oxidized, „M" – machined
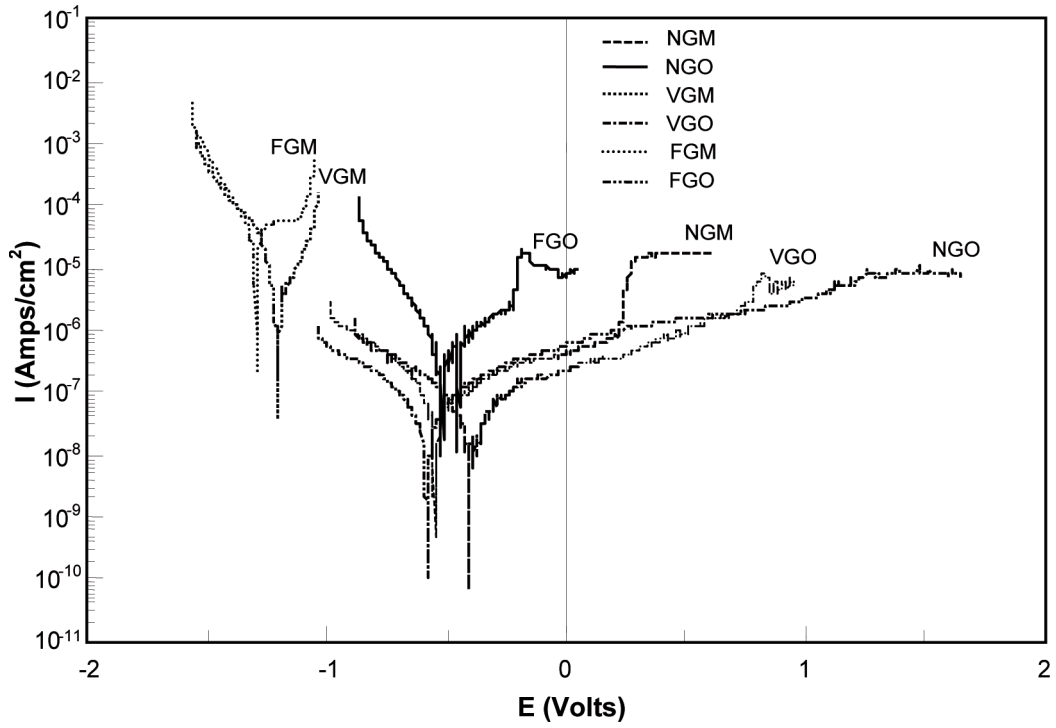
Fig. 9. The comparison of all registered polarization curves – labelling the same as at Fig. 7
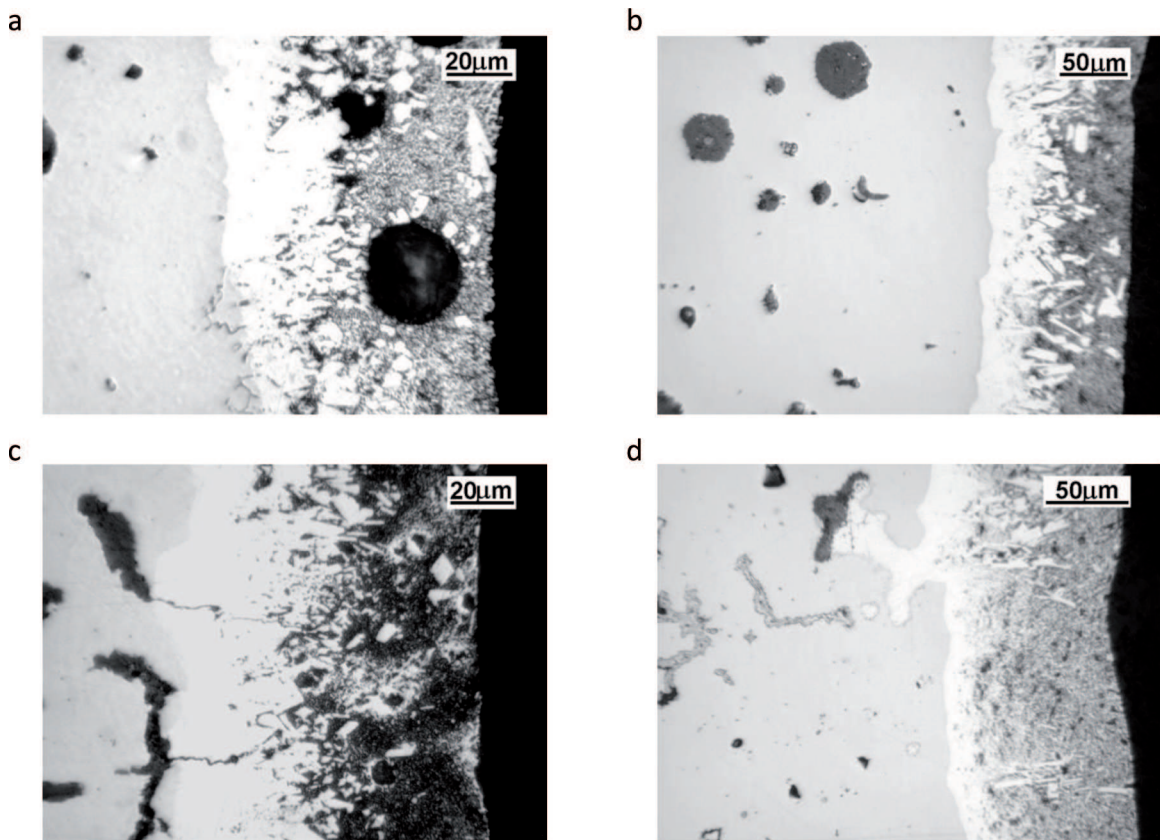

Fig. 10. Microstructure of cast iron observed after corrosion test: a, c – without oxidation; b, d – oxidized (a, b – nodular cast iron; c, d – cast iron with vermicular graphite)

All measured electrochemical parameters (corrosion potential E_{corr}, potential of cathode-anode pass E_{K-A}, polarization resistance R_p, corrosion current density i_{corr}) are presented in Table 1. Additionally values measured for steel 30MnB4 were put in the table to enable direct comparison of analogous data.

The comparison shows that oxidation process influences essentially the corrosion resistance of created zinc coating. It is manifested by decreasing the corrosion current density i_{corr} and increasing the corrosion potential E_{corr}. It regards especially cast iron with more developed graphite morphology, i.e.: cast iron with flake and vermicular graphite. The value of corrosion current density decreased in this case from $3,84 \cdot 10^{-5}$ to $5,14 \cdot 10^{-7}$ A/cm^2 in cast iron with flake graphite and from $3,91 \cdot 10^{-6}$ to $3,19 \cdot 10^{-8}$ A/cm^2 in cast iron with vermicular graphite. Whereas, value of corrosion potential increased correspondingly from -1070 to -371 mV and -1050 to -389 mV. It results mainly from elimination of negative influence of graphite exerting on the coating tightness.

Essential in this case is fact that vermicular and flake graphite precipitates frequently penetrate far more in coated zinc layer than nodular graphite and can in this way reduce its tightness in higher level (Fig. 1, 10). Such situation is not observed in case of oxidized cast iron. Cast iron, where the scale layer was removed only mechanically – using sandblasting, does not reveal deep zinc penetration inside the "after-graphite" pores – it reaches about 15μm.

Only when the chemical processing was used – dipping in solution of oxalic acid, the penetration depth considerable increases and achieves 120μm in cast iron with vermicular and flake graphite.

In cast iron with nodular graphite, the depth of zinc penetration is considerable smaller, and resolves itself into filling the pores situated near the outside surface. Also in this case the filled with zinc precipitation can be observed even in distance 75μm from the surface.

In case of nodular cast iron the differences between parameters i_{corr} and E_{corr} measured for oxidized and not subjected to such processing samples are slight ($i_{corr} = 2,72 \cdot 10^{-8}$; $5,27 \cdot 10^{-8}$ A/cm^2; $E_{corr} = -543, -580$ mV), but also in this case the course of anodic polarization confirms better coating passivation. The reason of such samples behaviour is on one hand smaller influence of nodular graphite on compactness of zinc coating, on the other hand too short time of oxidation, that was set and fixed for all samples in comparative purpose. As the effect single graphite precipitates were observed in subsurface layer of cast iron even after oxidation (Fig. 5c). For this kind of cast iron the oxidation time should be longer and amounts above 8h.

Considering the course of polarization curves the tested samples can be divided into two groups: with lower Zn layer corrosion resistance – cast iron samples galvanized after machining (except nodular cast iron) and higher Zn layer corrosion resistance – samples galvanized with prior oxidation.

Taking into account diversity of chemical composition of tested cast iron kinds, i.e. higher silicon content in cast iron with vermicular and nodular graphite and higher content of P, S and Mn in cast iron with flake graphite and influence of mentioned elements on structure and corrosion resistance of Zn layer at the iron alloys surface, it is evident that the dominating factor deciding on the quality of coating created at cast iron surface after machining is presence and form of graphite precipitates.

Because electrochemical parameters measured for zinc coating created at cast iron surface differ slightly from these measured in case of steel 30MnB4, we can't expect the significant improvement of zinc coating corrosion resistance as the effect of further optimization of oxidation process.

4. Conclusions

1. The oxidation process influences essentially the corrosion resistance of created zinc coating. It is manifested by both decrease the corrosion current density i_{corr} and higher value of corrosion potential E_{corr}.
2. The increase of corrosion resistance of Zn coating created after oxidation of cast iron with vermicular and flake graphite is much higher than in the case of nodular cast iron. In nodular cast iron the differences between parameters i_{corr} and E_{corr} measured for oxidized and not subjected to such processing samples are slight. In the case of nodular cast iron, the course of anodic polarization confirms better the coating passivation.
3. In practice, applied parameters of oxidation process should be dependent on kind of cast iron and selected basing upon individual requirements, elaborated kinetics of oxidation and creation of porous layer. In the case of tested materials, for assumed thickness of porous layer – 200μm, time of oxidation at 850°C should amounts to: 2; 2,5 and 8h, correspondingly to cast iron with flake, vermicular and nodular graphite.
4. The dominating factor which decides on the quality of coating created on cast iron surface is the presence and form of graphite precipitates. Higher silicon content in cast iron with vermicular and nodular graphite and higher content of P, S and Mn in cast iron with flake graphite and their influence on structure and corrosion resistance of Zn coating both were taken into account in the above conclusion.

154

5. Proposed method of treatment: oxidation combined with hot-dip zinc galvanizing enables achieving surface with better corrosion resistance and roughness. Roughness values measured after oxidation are sometimes even lower than these determined for zinc coating of cast iron after machining. It results first from negative influence of graphite precipitates uncovered during machining that can change locally the thickness and structure of coated layer and decrease in this way its tightness.

6. Two stages procedure of the scale layer removal: mechanical and chemical is necessary to obtain the desired result: formation of the composite subsurface layer and increase in Zn diffusion depth.

REFERENCES

[1] F.C. P o r t e r, 10th Eur. Corros. Congr., Barcelona, 687-690 (1993).

[2] D. K o p y c i n s k i, E. G u z i k, W. W o l c z y n s k i, Materials Engineering **4**, 1081-1084 (2006).

[3] D. K o p y c i n s k i, Monograph, AGH Kraków 2006.

[4] K. K u r s k i, Cynkowanie ogniowe. Warszawa, WNT 1970.

[5] N. D r e u l l e, P. D r e u l l e, J.C. V a c h e r, Metall **34**, 834-838 (1980).

[6] J. P e l e r i n, J. H o f f m a n n, V. L e r o y, Metall **35**, 879-873 (1981).

[7] H. W o z n i c a, L. B a r y l a, Acta Metallurgica Slovaca **8**, 355-360 (2002).

[8] L. S z i r a k i, E. S z o c s, Z. P i l b a t h, K. P a p p, E. K a l m a n, Electrochimica Acta **46**, 509-513 (2001).

[9] D. M y s z k a, Archives of Metallurgy and Materials **52**, 3, 475-480 (2007).

[10] T. G l a d m a n, B. H o l m e s, F.B. P i c k e r i n g, Journal Iron Steel Instr. **211**, 765-772 (1973).

[11] R.W. S a n d e l i n, Wire and wire product **15**, 655-660 (1940).

[12] H. G u t t m a n, P. N i e s s e n, Canadian Metallurgical Quartely **11**, 609-614 (1972).

[13] D. K o p y c i n s k i, E. G u z i k, W. W o l c z y n s k i, Materials Engineering **4**, 289-292 (2008).

[14] J. B a n a s, E. Guzik, D. K o p y c i n s k i, U. L e l e k - B o r k o w s k a, M. S t a r o w i c z, Materials Engineering **3-4**, 750-756 (2007).

[15] D. J e d r z e j c z y k, M. H a j d u g a, Archives of Metallurgy and Materials **56**, 4, 839-849 (2011).